Thermochimica Acta, 71 (1983) 15–24
Elsevier Science Publishers B V., Amsterdam – Printed in The Netherlands

COMPARATIVE STUDY OF THE THERMAL ANALYSES OF SOME TRANSITION METAL(II) PROPIONATES. PART I

P.S BASSI, H.S JAMWAL and B S RANDHAWA

Chemistry Department, Guru Nanak Dev University, Amritsar, Punjab (India)

(Received 1 June 1983)

ABSTRACT

The thermal decomposition of the propionates of Co(II), Ni(II), Cu(II) and Zn(II) has been studied using non-isothermal techniques (DTG, DTA and TG). The final thermolysis products in all these compounds are the corresponding metal oxides as confirmed by chemical analysis and X-ray powder diffraction method. The TG data for dehydration were computerised to test the various decomposition models. the Erofeev–Avrami equation, i.e $[-\ln(1-\alpha)]^r$ with $r = \frac{1}{3}$ for a nucleation-and-growth-controlled mechanism, has been found to be the most suitable. Comparison of the T_i values led to the stability orders Zn > Co > Cu > Ni and Zn > Co > Ni > Cu, for dehydration and decomposition processes, respectively

INTRODUCTION

The thermal decomposition of transition metal carboxylates has attracted considerable attention because (i) the end products possess important electronic/surface properties, and (ii) the decomposition mechanism is of interest. For complex systems, a comparative study has proved more rewarding for determination of thermal stability. Derivative and simultaneous thermoanalytical methods of analysis in combination with other techniques have provided extremely useful information about the stages in a decomposition process and the stability of the reactants/intermediates. In continuation of our earlier work on the decomposition of carboxylates [1–3], we report a comparative study of the thermal decomposition of the propionates of cobalt(II), nickel(II), copper(II) and zinc(II). Determination of the mechanism of a given decomposition using only the best fit of an equation has often been contradicted [4]. Therefore, the most appropriate and physically feasible mechanism for the first step of dehydration of these propionates and the thermal stability for the first stage of dehydration and decomposition of these complexes is being reported.

0040-6031/83/$03.00

EXPERIMENTAL

Cobalt(II) propionate trihydrate was prepared by adding cobalt(II) carbonate to propionic acid in small amounts with constant stirring until effervescence ceased. The reaction mixture was allowed to stand at room temperature for several hours. After filtration of the clear solution, it was concentrated on a water bath till pinkish crystals appeared. The crystals were separated, washed with distilled water and dried in air after recrystallisation. Similarly, the propionates of nickel(II), copper(II) and zinc(II) were also prepared.

The composition of these compounds was established by chemical analysis and infrared spectroscopy. The percentage of cobalt, nickel, copper and zinc was determined gravimetrically [5]. The percentage of carbon and hydrogen was determined by microanalysis. Analytical data showing the percentage of metals, carbon and hydrogen are listed in Table 1.

The derivatographic study of these carboxylates was carried out by means of a Paulik-Paulik-Erdey MOM derivatograph (Hungary) using 200 mg of the sample at 200 mg sensitivity and at a heating rate of 10° $\min^{-1}$ in a static air atmosphere. The powder X-ray diffraction patterns of the final thermolysis products of Cu(II), Ni(II) and Zn(II) propionates were recorded using nickel-filtered $\mathrm{Cu}K_\alpha$ radiation. The computer analysis was performed on a TDC-316 computer (ECIL, India).

RESULTS AND DISCUSSION

Derivatographic study

The results discussed were obtained from the non-isothermal studies (DTG, DTA and TG) of the various metal(II) propionates.

(i) Cobalt(II) propionate trihydrate

Figure 1 shows the simultaneous DTA, DTG and TG curves of cobalt(II) propionate trihydrate. The DTG curve shows peaks with maxima at 380, 523 and at 610 K with a small dent at 618 K. The DTA curve shows two endothermic peaks at 393 and 528 K and two exotherms at 603 and 673 K. The arrest in the TG curve corresponding to the DTA peak at 393 K is at 7% weight loss, indicating the elimination of one molecule of water (calcd. loss = 6.9%). Dehydration of the sample is complete at 523 K as indicated by a weight loss of 20.0% from the TG curve (calcd. loss = 20.8%). The decomposition of the compound starts at 603 K and is complete at 723 K as shown by the DTA and DTG peaks. The observed loss in the TG curve at 723 K is 68.0%, corresponding to the formation of CoO (calcd. loss = 71.1%). The end-product was confirmed by chemical analysis to be CoO.

TABLE 1

Analytical data for metal(II) propionates

Compound		Metal(%)	C(%)	H(%)
$Co(C_2H_5COO)_2$ 3 H_2O				
	Found	22.7	28 0	6 2
	Calcd.	22.6	27 8	6 1
$Ni(C_2H_5COO)_2 \cdot H_2O$				
	Found	26.4	32 4	5 1
	Calcd	26 4	32 3	4 9
$Cu(C_2H_5COO)_2$ 0 5 H_2O				
	Found	29 1	33 0	5 1
	Calcd	29.1	32.9	5 0
$Zn(C_2H_5COO)_2$ H_2O				
	Found	28.6	31 4	4.5
	Calcd	28.5	31 3	4.3

(ii) Nickel(II) propionate monohydrate

Figure 2 represents the simultaneous DTG, DTA and TG curves of nickel(II) propionate monohydrate. The DTG curve shows peaks with max-

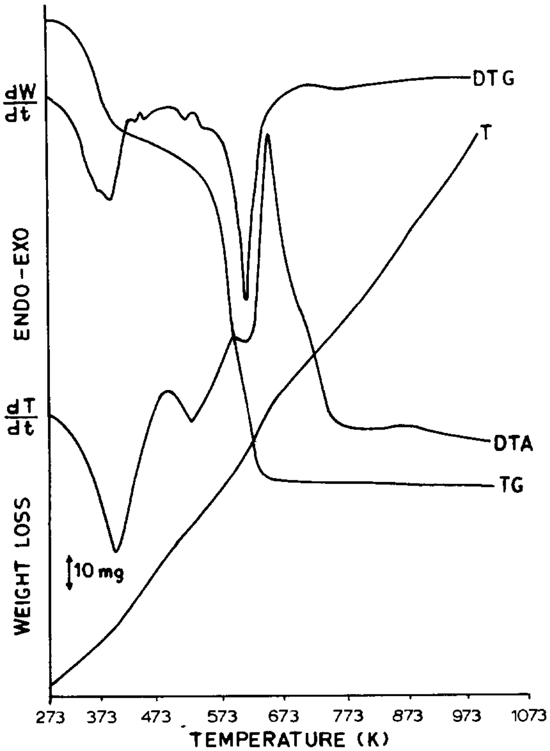

Fig. 1 Simultaneous DTG, DTA and TG curves of cobalt(II) propionate trihydrate at a heating rate of 10° min^{-1}

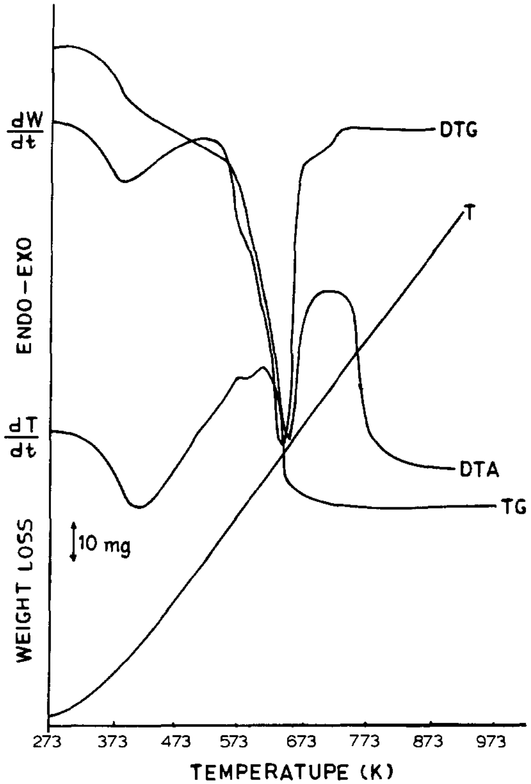

Fig 2 Simultaneous DTG, DTA and TG curves of nickel(II) propionate monohydrate at a heating rate of 10° min^{-1}

ima at 393, 573 and 648 K. The DTA curve shows an endotherm with peak maximum at 398 K and exothermic peaks at 573 and 613 K followed by a large exothermic region from 713 to 753 K. The DTG curve also shows peaks corresponding to all the stages shown by the DTA curve, indicating that all the thermal effects are accompanied by loss in weight. The first DTG peak is not symmetric and the corresponding DTA peak is broad, which indicates more than one step of decomposition. A change in slope of the TG curve at a loss of 8.0% is due to loss of one water molecule (calcd. loss = 8.1%). The exotherms at 573 and 613 K indicate that decomposition of the anhydrous sample has started. The weight loss from 713 to 753 K indicated by the DTG and DTA peaks suggests the formation of NiO. The TG curve shows a weight loss of 66.0% against the calculated loss of 66.5%. The formation of NiO as the ultimate product has been confirmed by chemical analysis and X-ray powder diffraction results [6].

(iii) Copper(II) propionate hemihydrate

Figure 3 shows the simultaneous DTG, DTA and TG curves of copper(II)

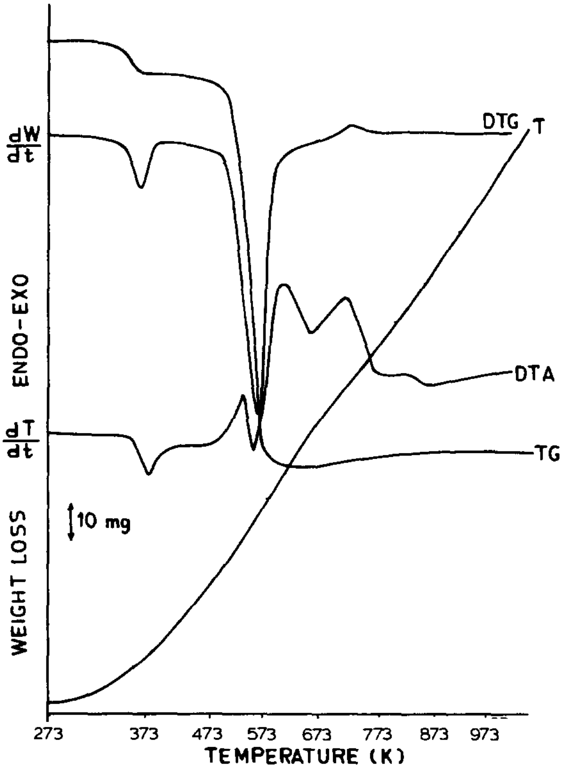

Fig 3. Simultaneous DTG, DTA and TG curves of copper(II) propionate hemihydrate at a heating rate of 10° min^{-1}

propionate hemihydrate. The DTA curve shows endothermic peaks at 368 and 813 K and exothermic peaks at 533, 603 and 703 K. The DTG curve shows two peaks with maxima at 363 and 548 K. The loss from the TG curve corresponding to the first endotherm in the DTA curve is 4.5%, due to the loss of half a water molecule (calcd. loss = 4.1%). The anhydrous sample remains quite stable up to 513 K and then its decomposition starts. Decomposition is completed at 703 K as shown by peaks in the DTG and DTA curves. The TG curve shows a weight loss of 63.0% indicating the formation of CuO (calcd. loss = 63.5%). The DTG and TG curves show that one decomposition reaction accompanied by weight loss takes place and no stable intermediate is formed. The final thermolysis product has been confirmed by chemical analysis and X-ray powder diffraction technique [7] to be CuO.

(iv) Zinc(II) propionate monohydrate

Figure 4 shows the simultaneous DTG, DTA and TG curves of zinc(II) propionate monohydrate. The DTG curve shows four peaks with maxima at 403, 553, 633 and 653 K. The DTA curve represents four endothermic peaks

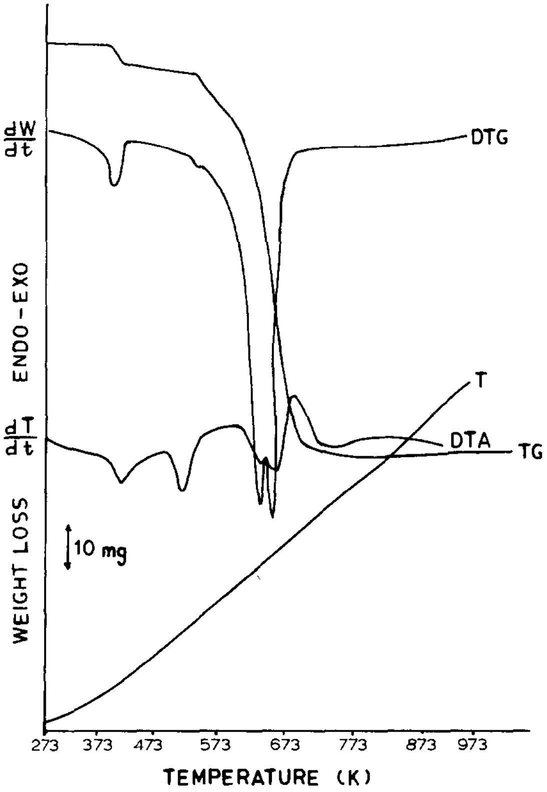

Fig 4 Simultaneous DTG, DTA and TG curves of zinc(II) propionate monohydrate at a heating rate of 10° min^{-1}

with maxima at 408, 513, 643 and 663 K. The endotherm at 663 K is immediately followed by an exothermic region from 673 to 733 K. The first stage in the TG curve shows a weight loss of 4.8% and then a further loss of 7.5% at 513 K indicating the elimination of one water molecule (calcd.

TABLE 2

X-Ray powder diffraction data for the final thermolysis product of nickel(II) propionate monohydrate

Experimental		ASTM data for NiO	
d(Å)	Intensity	*d*(Å)	Intensity
2 410	90	2 410	90
2 089	100	2 088	100
1 475	60	1 476	56
0 932	20	0 933	21

TABLE 3

X-Ray powder diffraction data of the final thermolysis product of copper(II) propionate hemihydrate

Experimental		ASTM data for CuO	
d(Å)	Intensity	*d*(Å)	Intensity
2 754	15	2 751	12
2.530	50	2 530	49
2 520	100	2.523	100
2 330	95	2.323	96
2 302	40	2.312	30
1 981	5	1 959	3
1 859	25	1 866	25
1 743	8	1.714	8
1 566	14	1 581	14

loss = 7.8%). The final weight loss in the TG curve at 733 K is 63.0 indicating the formation of ZnO (calcd. loss = 64.5%). The end-product of pyrolysis has been confirmed by chemical analysis and X-ray powder diffraction method [8] to be ZnO.

The identity of the final thermolysis products of the compounds was confirmed by comparing the *d* values and corresponding relative intensities from X-ray diffraction data with those given in the literature (ASTM data file). The X-ray diffraction parameters are given in Tables 2–4.

TABLE 4

X-Ray powder diffraction data for the final thermolysis product of zinc(II) propionate monohydrate

Experimental		ASTM data for ZnO	
d(Å)	Intensity	*d*(Å)	Intensity
2 814	80	2 820	76
2 816	60	2 816	56
2.610	100	2 620	100
2 476	30	2 476	29
1 911	40	1.911	40
1 626	35	1.626	35
1 470	8	1 470	6
1.400	27	1.400	28
1 370	3	1 370	3
1 300	5	1 300	5

TABLE 5

Computerised kinetic parameters for the dehydration step in the TG curve of cobalt(II) propionate trihydrate obtained by the Coats–Redfern equation, $\log[g(\alpha)/T^2]$ vs. $1/T$

$g(\alpha)=\int_0^{\alpha} d\alpha/f(\alpha)$

Model no	$g(\alpha)$		Energy, E (kcal mole^{-1})	Pre-exponential factor, z	Least-sq error	Chi-sq. error
1	$-\ln(1-\alpha)$		23.09	74744 640	0.015	0.119
2 (i)	$-\ln(1-\alpha)^r$,	$r=1/4$	3.28	0 577	0.375	0.031
(ii)		$r=1/3$	5.57	3.353	0 492	0.048
(iii)		$r=1/2$	10.08	68.844	0 728	0.060
(iv)		$r=2/3$	14.50	1071.349	0.966	0.079
3	$\ln(\alpha/1-\alpha)$		55 97	0.000	0.028	0.400
4	$3[1-(1-\alpha)^{1/3}]$		18.19	7340.08	0.016	0.123
5	$2[1-(1-\alpha)^{1/2}]$		16 40	2234.79	0.016	0.124
6 (i)	$r-(1-\alpha)^r$,	$r=2$	0 08	0.005	0.377	0.033
(ii)		$r=3$	1.40	0.054	0.234	0.021
(iii)		$r=4$	2 05	0.077	0.173	0.016
7 (i)	α^r,	$r=1/4$	0.60	0 020	0.409	0.034
(ii)		$r=1/3$	2.00	0.138	0.537	0.044
(iii)		$r=1/2$	4.74	1 280	0.795	0.064
(iv)		$r=1$	12.58	162.858	0.015	0.121
(v)		$r=3/2$	19.87	9299.219	0 023	0.176
(vi)		$r=2$	26.67	51247.68	0 032	0.228
8	$3/2[1-(1+\alpha)^{1/3}]^2$		37.80	52784.00	0.031	0 209
9	$3/2[(1+\alpha)^{1/3}-1]^2$		24.55	12023.01	0.029	0.185
10	$3/2[1-3/2\alpha-(1-\alpha)]^{3/2}$		33.06	34305.60	0.032	0.210
11	$(1-\alpha)\ln(1-\alpha)+\alpha$		30.67	77988.80	0.033	0.226
12 (i)	$\ln\alpha^r$,	$r=1$	41.36	0.000	0 028	0.174
(ii)		$r=2$	41 20	0.000	0 028	0.182

COMPARATIVE STUDY OF THE THERMAL ANALYSES

As shown by the derivatographic study, the decomposition of hydrated metal(II) propionates occurs in stages, dehydration being an endothermic process. Comparison of the T_i values of dehydration shows the stability order: Zn > Co > Cu > Ni, which is not in agreement with the order obtained from the corresponding T_m values. Since T_i values provide more accurate information about the thermal stability of the propionates, it has been preferred.

The activation energy for the dehydration stage was computed from TG data using the Coats–Redfern equation to which all the known models of decomposition were applied. The computerised kinetic parameters for the dehydration of cobalt(II) propionate trihydrate are listed in Table 5. Keeping in view the least-squares-method error and the chi-square error, it is very difficult to decide as to which model will apply in a given decomposition process. The kinetic model 6(iii) with $r = 4$ (given in Table 5) provides the least value of chi-square error but it is not a physically feasible model. The results obtained from isothermal study of the dehydration of these samples give sufficient evidence for a nucleation-and-growth-controlled mechanism for which the Erofeev–Avrami equation holds good. Of the various values of this equation, the most appropriate one which is physically feasible and has very little computer error is $[-\ln(1-\alpha)]^r$ with $r = \frac{1}{3}$: it also provides a reasonable energy of activation for dehydration. The same equation has also been found to be the most satisfactory in the case of nickel, copper and zinc propionates with activation energies of 3.39, 18.05 and 10.56 kcal mole^{-1}, respectively. On the basis of activation energy considerations, the order of thermal stability observed was: Cu > Zn > Co > Ni.

For decomposition, comparison of T_i and T_m values (Table 6) shows the same order of thermal stability: Zn > Co > Ni > Cu.

However, Irving and Williams [9] reported the following order of stability for various organic ligands coordinated to the transition metal, by taking ionisation potential and entropy changes into account: Co < Ni < Cu > Zn.

From the computer analysis, it has been observed that the same result

TABLE 6

T_i and T_m values for the dehydration and decomposition of various transition metal(II) propionates

Compound	Dehydration		Decomposition	
	T_i	T_m	T_i	T_m
$Co(C_2H_5COO)_2\cdot 3\ H_2O$	353	380	573	623
$Ni(C_2H_5COO)_2\cdot H_2O$	343	393	558	573
$Cu(C_2H_5COO)_2\cdot 0.5\ H_2O$	348	363	528	548
$Zn(C_2H_5COO)_2\ H_2O$	376	403	598	633

when applied to different equations, produces a large difference in activation energy in spite of the feasibility of these equations regarding the magnitude of chi-square and least-squares-method errors. In all the decomposition processes except that of zinc(II) propionate, there is a small gain in weight at the last stage which is due to the taking up of oxygen by the reduced metal.

REFERENCES

1 P.S Bassi and P.C. Kalsi, Indian J Chem., 14A (1976) 967.
2 P S Bassi and P.C. Kalsi, J. Therm. Anal, 13 (1978) 363.
3 P C Kalsi, P.S. Bassi and C.M. Khajuria, Thermochim Acta, 41 (1980) 265.
4 D Dollimore and N.M. Guindy, Thermochim Acta, 58 (1982) 191.
5 I.A. Vogel, Quantitative Inorganic Analysis, Longmans Green, London, 1962, pp 479, 497, 531, 533
6 X-Ray Diffraction Data for NiO, ASTM Card No. 4-0835
7 X-Ray Diffraction Data for CuO, ASTM Card No 5-0661
8 H E. Swanson and R.K. Fuyat, Natl. Bur. Stand (U.S.) Circ 539, Vol 2, 1953, p 65
9 H Irving and R.J P. Williams, J Chem. Soc, (1953) 3192